JOURNAL OF MECHANICAL AND TRANSPORT ENGINEERING
Vol. 69, No. 3 2017
DOI 10.21008/j.2449-920X.2017.69.3.03

Damian JOACHIMIAK*
Piotr KRZYŚLAK*
(Received: 5 MAY 2015, Received in revised form: 9 MAY 2017, Accepted: 11 MAY 2017)

DESCRIPTION OF A TEST STAND AND MEASUREMENT EQUIPMENT FOR LABYRINTH SEAL TESTING

The paper presents a test stand for testing segments of single sided and double-sided labyrinth seals. The geometry of the test stand has been designed and constructed by the authors of the paper. The elements and the design of the test stand allow investigations of the seal for a variety of initial pressures with the measurement of the mass flow in the inlet and outlet channels. The design of the test stand enables testing seal segments with a turbulent flow. The geometry of the mating pairs of single and double-sided seals allows a measurement of the pressure in selected chambers of the seal chambers.

Keywords: labyrinth seals, fluid-flow machines, diagnostics, leakage

1. INTRODUCTION

The test stand presented in the paper serves the purpose of investigating the behavior of a seal segment with a turbulent flow under laboratory conditions. Thus far, in literature [Timpton 1985, Witting 1987, Anker 2002, Gamal 2007, Vakili 2015, Joachimiak 2013, Li 2013, Hu 2014] no information has been provided on the testing of segments of labyrinth seals composed of several discs: single-, double sided and slotted labyrinth seals. The test stand has been designed based on calculations included in works [Joachimiak 2013, Joachimiak et al. 2013, Joachimiak 2011]. The pressure supply to the test stand allows testing segments for varied initial pressures in the range of $p_0 = 1.1 - 4 \cdot 10^5$ Pa at final pressures approximating that of ambient pressure. The design of the test stand allows testing the behavior of a segment of a seal

* Faculty of Machines and Transport, Poznan University of Technology.

with a turbulent flow according to the co-author's novel idea claimed with a patent [Krzyślak and Winowiecki 2006]. In work [Krzyślak 2018], theoretical assumptions related to the diagnostic methods of labyrinth seals have been described.

2. DESIGN OF THE TEST STAND

The test stand for investigating labyrinth seals (Fig.1.) is powered with compressed air accumulated in two tanks: the compressor tank and the main tank, of the volume of 3 m^3 and 0.5 m^3 respectively, coupled in series. The tanks are filled by a two-stage piston compressor of the maximum compressing pressure of $p_{max} = 1.5 \cdot 10^5$ Pa. The system of tanks is secured against excess pressure with a safety valve. The pressure flowing out of the cylinder is reduced by a linear regulator. The main elements of the test stand are: the inlet part, the body, the outlet channel and the drain collector.

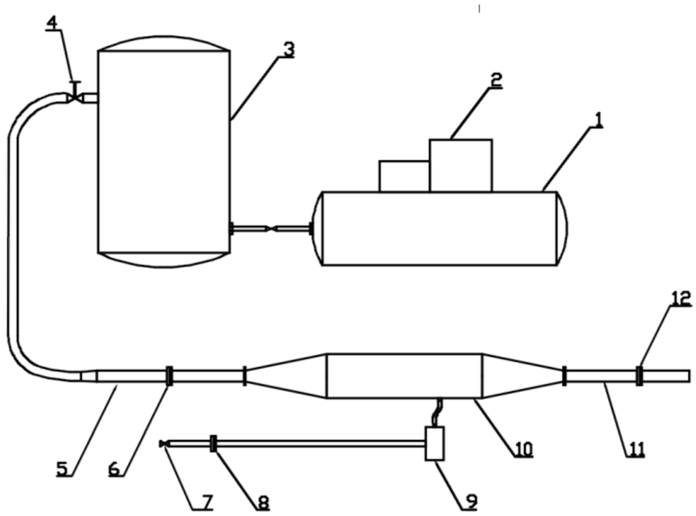

Fig. 1. Diagram of the test stand for testing labyrinth seals, 1– compressor tank, 2 – compressor, 3 – main tank, 4 – regulator valve, 5 – inlet channel, 6 – orifice 0, 7 – drain valve, 8 – orifice 1, 9 – drain collector, 10 – model of segment labyrinth seal, 11 – outlet channel, 12 – orifice

The inlet part of the test stand consists of a regulator valve and the inlet channel that supplies air to the measurement orifice 0 (Fig. 2) and then to the diffuser.

Fig. 2. The inlet part of the test stand: 1 – main cylinder, 2 – regulator valve, 3 – inlet channel

The diffuser and the confusor are fixed to the body presented in Fig. 3. On the surface of the body there are spouts allowing the connection of the pressure converters and thermoelements.

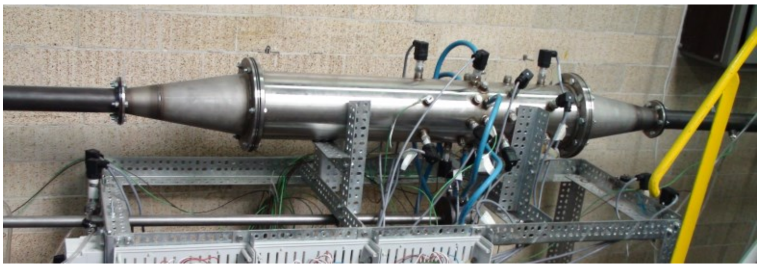

Fig. 3. Main body fitted on the test stand

Figure 4 shows the longitudinal cross-section of the body and three transverse cross-sections: 0, 1, 2 which are at the same time the measurement cross-sections. These cross-sections are in the transverse planes against the axis: upstream of the stuffing box segment at the point of the drain and downstream of the stuffing box segment. The design of the body allows measurement of the static pressure in each of the chambers through 18 spouts shown in plane A (Fig. 4) located spirally on the outer surface between cross-sections 0-1 and 1-2 (Fig. 3). Six spouts located in the central plane are for channeling gas from the stuffing box to the drain collector (Fig. 6).

The inner part is located centrically in the body. It forms the inner part of the model of labyrinth seal (Fig. 5). It is fixed to the body with supporting discs (front and rear) as shown in Fig. 5. For precise fixing of the inner part, both discs are equipped with locks. The front disc supports the inner part and fixes it axially. The rear disc sets the inner part axially and transversely through a distance sleeve. This solution allows alignment of the inner part against the body and the drain point.

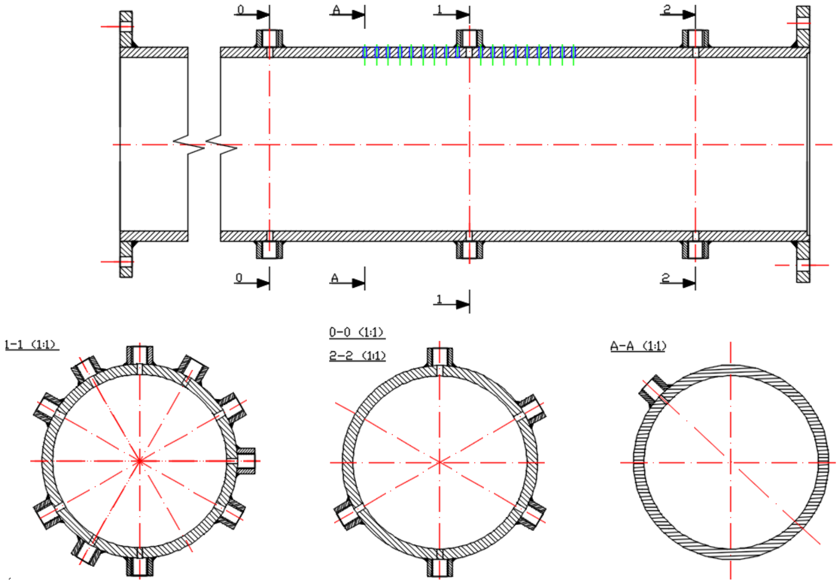

Fig. 4. Overview of the body, longitudinal and transverse cross-sections of measurement planes 0, 1, 2 and eight planes A

a) b)

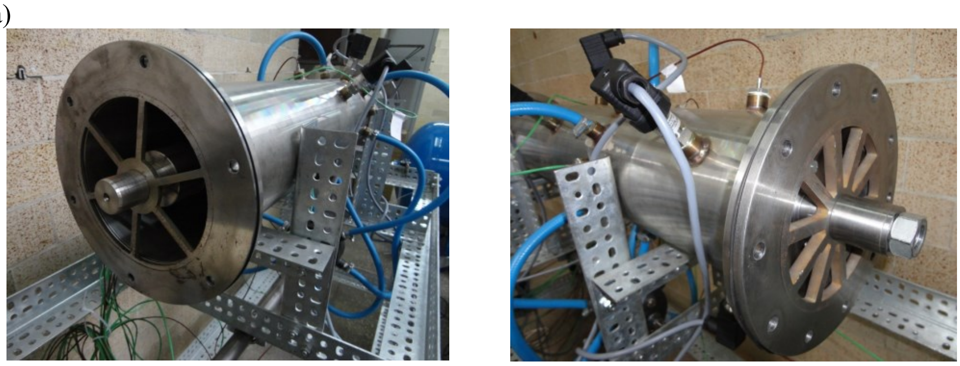

Fig. 5. Supporting discs fitted on the test stand, a) front, b) rear

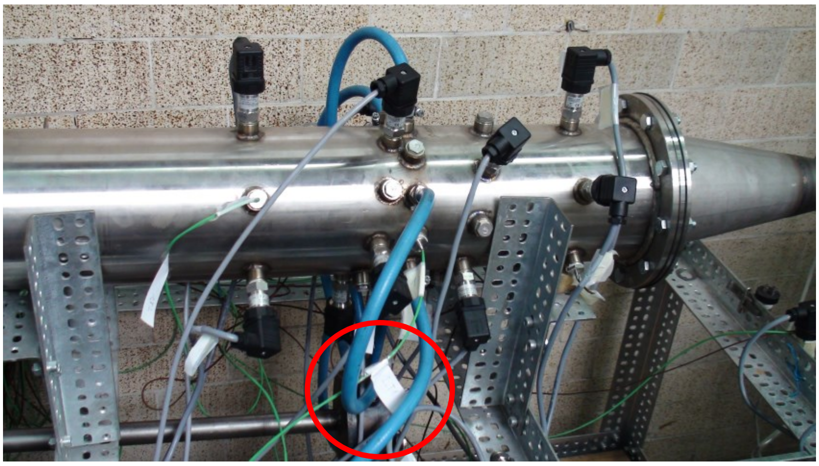

Fig. 6. Connection of the spouts in the body to the drain collector

The inner part presented in Fig. 2.7 is composed of a cylindrical part on which the distance sleeves are put and a set of discs. The discs and the sleeves are fixed by a pressing element in the rear of the inner part. Changing the distance sleeves allows alignment of the discs against the inner part. Discs of different geometry can be fixed on the inner part. The calibration of the stuffing box can also be modified by changing the size of the distance sleeves.

a)

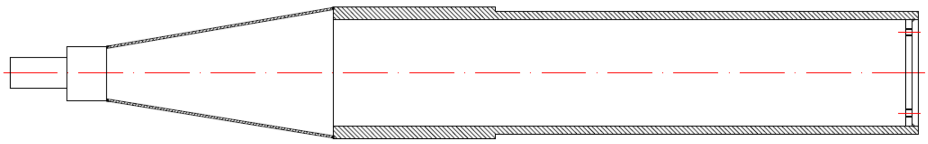

b)

Fig. 7. The inner part of a single-sided seal: a) overview, b) image of the inner part with the discs and distance sleeves

The geometry of the external distance sleeves fitted in the inner part of the double-sided seal (Fig. 8) allows a measurement of the pressure distribution inside the chambers between the seal discs.

a)

b)

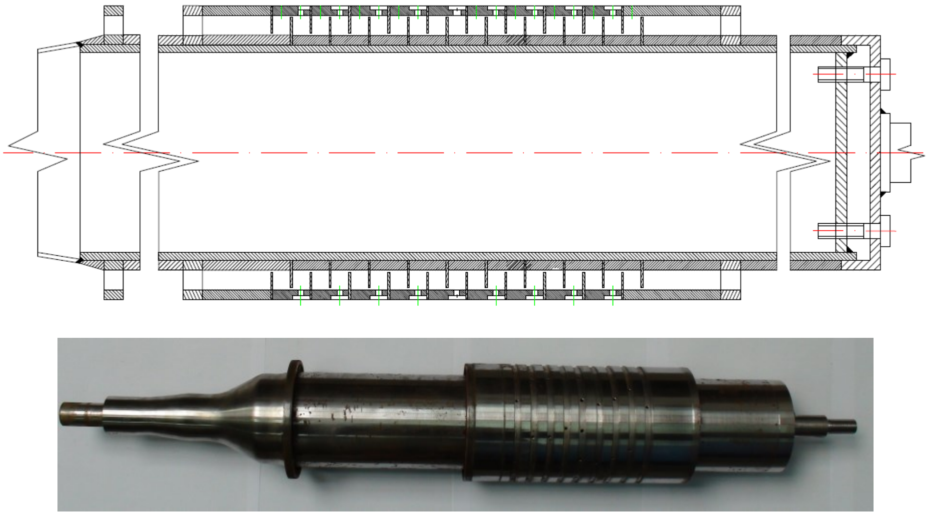

Fig. 8. The inner part of a double-sided seal: a) overview, b) image of the inner part with the discs on and internal and external sleeves on

The shape of the diffuser and the shape of the front of the inner part ensures an equal distribution of air in the circumference when coming into the stuffing box. The front supporting disc (Fig. 5a) is made in such a way as to minimize the turbulence in the airflow. The cylindrical part before the stuffing box reduces the turbulence rate of the flowing air. At this point, a measurement is made of the static pressure and temperature of air flowing to the seal model (cross-section 0, Fig. 4). Downstream of the stuffing box there is a cylindrical outflow part at which a measurement is made of the static pressure and temperature of air flowing out of the segment (cross-section 2, Fig. 4). Downstream of the segment and the rear disc a confusor is fitted whose role is to reduce the turbulence in the airflow coming out of the stuffing box and going through the rear supporting disc (Fig. 5b). The outlet part is made of a confusor and an outlet channel where the measurement orifice 2 is fitted.

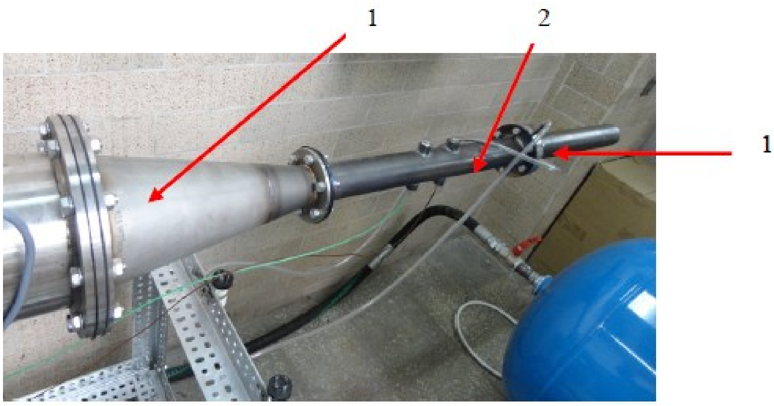

Fig. 9. The outlet part: 1 – the confusor, 2 – the outlet channel, 3 – orifice II

Hoses channeling the gas from the labyrinth stuffing box are fixed to the drain collector (Fig. 6 and 10). In the final part of the outlet channel from the confusor, orifice 3 is fitted for the measurement of the channeled gas. The geometries of the inlet and outlet channels have been designed in compliance with standard [PN-EN ISO 5167-1].

Fig. 10. Drain collector

3. MEASUREMENT SYSTEM

The measurements of the mass flow are made with the orifices with a near-disc pressure takeoff (Fig. 11.). The orifices are made to Polish Standard specification [PN-EN ISO 5167-1]. During the measurements, in order to balance the mass flow, geometrical similarity of orifices 0 and 2 was applied. As recommended in [PN-EN ISO 5167-1], stabilizing segments have been added before the orifices.

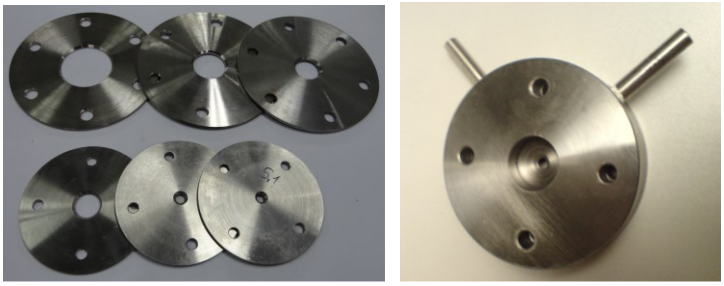

Fig. 11. The orifices used in the tests and measurements of the test stand, elements for the measurement of the pressure near the disc

Figure 12 presents the geometry of the channel of the pressure takeoff disc and the orifice fitted on the test stand. They were symbol-dimensioned. The values of the individual dimensions are provided in Table 1.

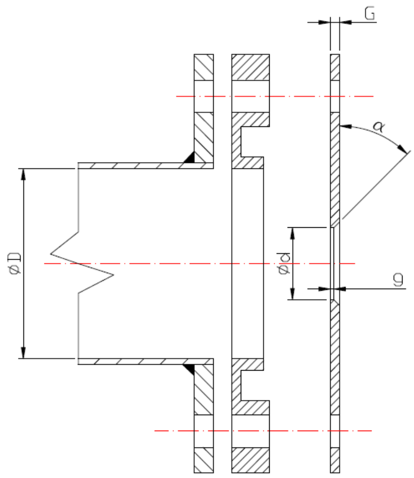

Fig. 12. The geometry of the pressure takeoff channels and orifices used on the test stand

Table 1 contains the dimensions of the orifices and channels in the individual measurement points of the mass flow.

For the pressure measurement piezoresistant voltage signal absolute pressure converters have been used (PAA-23SY) (Fig. 13a). The measurement range of the converters is $0\text{-}5{\cdot}10^5$ Pa. The accuracy of this type of converter is 0.25% of the measurement range. The difference pressure on the orifices is measured with PD-23 converters (Fig. 13b) of the ranges of $0\text{-}0.25{\cdot}10^5$ Pa and $0\text{-}1{\cdot}10^5$ Pa. The measurement accuracy of the PD-23 converter is 0.2% of the measurement range.

Table 1

Geometries of the channels and orifices at the mass flow measurement points (Fig. 2.1)

Symbol	Description	Orifice 0	Orifice 1	Orifice 2
D	pipeline diameter [mm]	50	50	20
d	chokepoint diameter [mm]	17 25 37.5	19 25	4 5.1 6
α	bevel angle [º]	45	45	45
G	orifice thickness [mm]	2.5	2.5	2.5
g	chokepoint thick-ness [mm]	1	1	1

The temperature measurements were made with T thermocouples (Fig. 13 c). Under the measurement conditions water can condense in the decompressing air, hence the thermocouple joints were covered with PTFE. The PTFE layer also protects the thermocouple against mechanical damage. Each of the thermocouples was fixed in a spout allowing airtight fitting. The geometry of the thermocouple spout was selected so that the joint was near the surface of the channel wall.

Fig. 13. Measurement equipment: pressure converters; a) absolute pressure converter PAA-23SY, b) difference pressure converter PD-23, c) PTFE covered T thermocouple

The geometry of the body allows detecting pressure in twenty-one measurement planes (Fig. 4). During the measurement, the pressure values are recorded from several measurement points and the temperature values from ten measurement points. Figure 14 shows the spots where the static pressure is measured in the seal chambers.

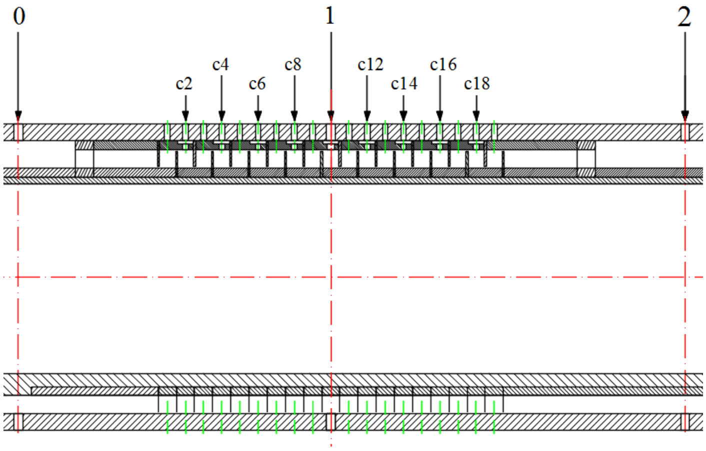

Fig. 14. Diagram of the location of the measurement planes: 0, 1, 2 and the points of measurement of static pressure in the chambers of single-sided and double-sided seals

In order to pull the measurement data during the experiment with appropriate frequency (depending on the type of measurement), two measurement lines were nstalled. The first one was based on the Adam series modules and the other on the National Instruments platform.

4. MEASUREMENT SYSTEM

The measurement system is based on two architectures. The first is composed of the Adam series modules (Fig. 15). Modules 4117 also have voltage inputs and support the pressure converters. For the measurement of the temperature, modules 4118 were used. The said modules support the USB-RS232 converter. Technical specifications of these devices have been included in [Joachimiak 2013]. The Adam series modules were configured in AdamView.

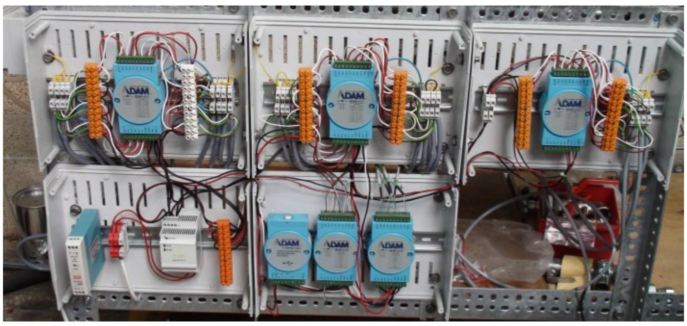

Fig. 15. Adam series 4117 and 4118 modules, USB-RS232 converter and the adapters

The basis of the other measurement system is the NI PXIe-1073 control platform supporting the NI PXIe-6341 card of voltage and current inputs and outputs and the NI TB-4353 card for thermocouples (Fig. 16). This system is characterized by a high frequency of the pulled data. The platform and the measurement cards of this system were configured in LabView.

Fig. 16. NI PXIe-1073 control platform with NI PXIe-6341 and NI TB-4353 cards

LabView and AdamView software used in the test stand allows a detection of the fitted measurement converters and thermocouples. The software allows setting the type and value of the range of the measurement signal from the pressure converters and determining the type of each of the connected thermocouples. The used software enables storage of data in the form of tables in text files.

$$\dot{\imath} \qquad \cdot \qquad \cdot \tag{1}$$

where:

$\dot{\imath}$ – the mass flow on orifices 0,

$\dot{\imath}$ – the mass flow on orifices 1,

$\dot{\imath}$ – the mass flow on orifices 2 [kg/s].

An example course of the mass flow changes on orifices 0, 1 and 2 has been shown in Fig. 17.

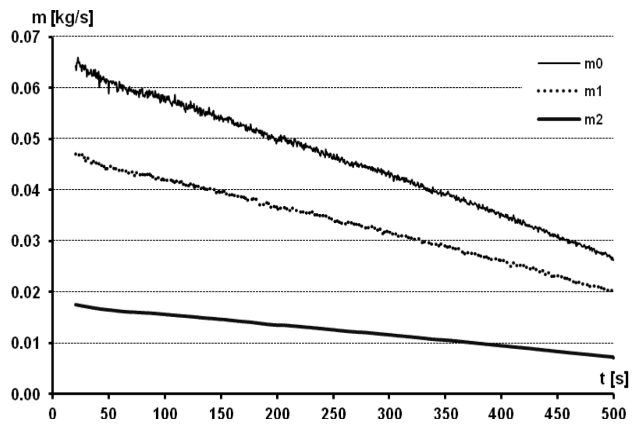

Fig. 17. Values of the changes of mass flow in orifices 0, 1 and 2 during the measurement

The accuracy of the balance of mass flow on the test stand is defined as follows:

$$\delta \dot{m} \qquad \%. \tag{2}$$

The design of the test stand presented in the paper and the measurement system allow calculating the mass flow for each measurement unit in the inlet, outlet and drain collector channels [Krzyślak 2008, Krzyślak and Winowiecki 2006].

In the tests of the stuffing box without a drain valve an average accuracy of the mass flow measurement was on the level of 2.1% (Fig. 18). For the stuffing box with the drain valve fitted the accuracy was on the level of 2÷4%.

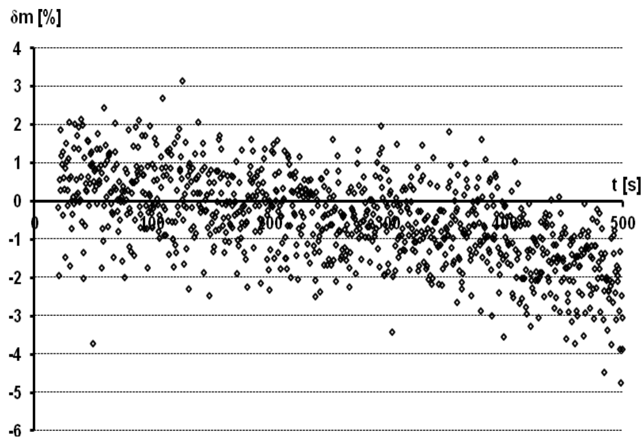

Fig. 18. Relative difference of the mass flow in the inlet and outlet channels

Figure 19 shows the distribution of pressure in the seal chambers during the measurement in the measuring points shown in Fig. 14.

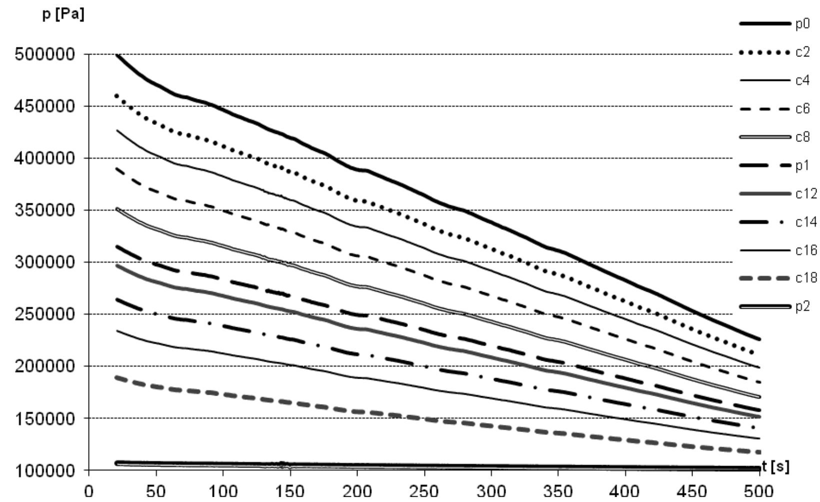

Fig. 19. Values of the static pressures in the single-sided seal channels

The data from the ‘Kryza’ software (Fig. 17–19) are subject to processing by DSV software [Joachimiak 2011, Joachimiak 2013] and are compared with the results of theoretical calculations.

6. CONCLUSIONS

When designing the tests stand, thermodynamic and flow conditions were estimated occurring upstream and downstream of the segment. Based on these assumptions, the values of the mass flow going through the stuffing box models were calculated. On this basis, the diameters of the inlet and outlet channels were determined along with the geometry of the orifices and the thermodynamic values of the gases at the orifices. The results presented in chapter 5 confirm an appropriate design of the test stand. Most importantly, an acceptable value of parameter $\delta_{\dot{I}}$ was obtained (Fig. 18) specifying the accuracy of the balancing of the mass flow on the test stand (equation 2). An almost constant percentage value of the drained mass flow was obtained. The compressed high capacity air cylinders used in the test stand ensured a low drop of pressure at the inlet to the seals during the measurement.

The investigations performed thus far within the grant no. NN513 324 740 resulted in many interesting observations and conclusions on the phenomena occurring during gas flow in the seals of different geometries and varied deterioration. Currently, works are planned on the development of new elements of the test stand allowing more detailed investigations of the phenomena occurring in different geometries of labyrinth stuffing boxes.

REFERENCES

Anker J., Jürgen F., Stetter H., 2002, Computational Study of the Flow in an Axial Turbine with Emphasis on the Interaction of Labyrinth Seal Leakage Flow and Main Flow, E. Krause et al. (eds.), High Performance Computing in Science and Engineering 2001, Springer-Verlag, Berlin Heidelberg.

Gamal Eldin A.M., 2007, Leakage and rotordynamic effects of pocket damper seals and see-through labyrinth seals, PhD thesis, Texas A&M University, USA.

Hu D., Jia L., Yang L., 2014, Dimensional Analysis on Resistance Characteristics of Labyrinth Seals, Journal of Thermal Science Vol. 23, No. 6, p. 516–522.

Joachimiak D., 2013, The labyrinth seals research with extraction. PhD thesis, Poznan University of Technology, Poznan.

Joachimiak D., Joachimiak M., Krzyślak P., 2013, The analysis of the calculation process related to labyrinth sealing with extraction, International Journal of Applied Mechanics and Engineering, Vol. 18, 4, p. 1057–1067.

Joachimiak D., Krzyślak P., 2011, Analysis behavior of labyrinth seal changes due to gas supply thermodynamic parameters, in: The 1st International Congress on Thermodynamics, Poznań, 4–7.09.2011, p. 795–804.

Joachimiak D., Krzyślak P., 2011, Calculation of labyrinth seals with extraction, International Journal o Applied Mechanics and Engineering, Vol. 16, 1, p. 5–14.

Joachimiak D., Joachimiak M., Krzyślak P., 2013, Description program Dławnica used for calculations labyrinth seals, Journal of Mechanical and Transport Engineering, Vol. 65, 1, p. 25–35, (in Polish).

Joachimiak D., Krzyślak P., 2011, Porównanie jednowymiarowych modeli obliczeniowych przepływu ściśliwego i nieściśliwego płynu w dławnicy labiryntowej, Zeszyty Naukowe Politechniki Poznańskiej, seria Maszyny Robocze i Transport, 2011, nr 64.

Krzyślak P., 2008, A method of diagnosing labyrinth seals in fluid-flow machines, Polish Maritime Research, Vol. 15, 3 (57), p. 38–41.

Krzyślak P., Winowiecki M., 2006, RP Patent Office: P-379431 – acknowledgement of patent submission. Flow seal in a fluid-flow machine and method of its diagnostics, Warsaw, (in Polish).

Li J. et al., 2013, Experimental and numerical investigations on the leakage flow characteristics of labyrinth seals, in: Heat Mass Transfer and Energy Conversion, Conf. Proc. 1547, p. 164–172.

PN-EN ISO 5167-1: Pomiary strumienia płynu za pomocą zwężek pomiarowych wbudowanych w całkowicie wypełnione rurociągi o przekroju kołowym, Warszawa 2005.

Tipton D.L., Scott T.E., Vogel T.E., 1985, Analytical and experimental development of a design model for labyrinth seals, Air force wright aeronautical laboratories, Allison Gas Turbine-Division of General Motors Corporation, USA.

Wittig S. et al., 1987, Numerical predictions and measurements of discharge coefficients in labyrinth seals, ASME 87-GT-188, p. 1–6.

Vakili D., Meganathan A., 2005, An Experimental and Numerical Study of Labyrinth Seal Flow, in: Proceedings of the Asme Turbo Expo, Vol. 3, Part B, p. 1121–1128.

OPIS STANOWISKA I SYSTEMU POMIAROWEGO DO BADAŃ USZCZELNIEŃ LABIRYNTOWYCH

Streszczenie

W artykule przedstawiono stanowisko do badań segmentów uszczelnień labiryntowych jednostronnych i dwustronnych. Geometria stanowiska została zaprojektowana i wykonana przez autorów. Elementy i konstrukcja stanowiska umożliwiają przeprowadzenie badań uszczelnienia z uwzględnieniem różnych zakresów ciśnienia początkowego z pomiarem strumienia masy w kanale dopływowym i kanałach wypływowych. Konstrukcja stanowiska umożliwia badanie segmentów uszczelnień z zaburzonym przepływem. Geometria korpusu i wsadu uszczelnień jednostronnego i dwustronnego umożliwia pomiar ciśnienia w wybranych komorach uszczelnienia.

Słowa kluczowe: uszczelnienia labiryntowe, maszyny przepływowe, diagnozowanie, przeciek